Evaluating Tropical Chlorophyll-a Algorithms from Sentinel-2 Satellite Imagery: A Comparative Study with In Situ Observation Data in Freshwater Bodies of Thailand

Rakasachat, C.,[1] Chaichana, R.,[1*] Phonmat, P.,[1] Klongvessa, P.,[1] Moukomla, S.,[2] Chanthorn, W.[1] and Bruun, T. B.[3]

[1]Department of Environmental Technology and Management, Faculty of Environment, Kasetsart University, Thailand, E-mail: chuti.r@ku.th, fscircc@ku.ac.th,* peangtawan.p@ku.th, ecpwk@ku.ac.th, wirongc@yahoo.com

[2]Department of Geography, Faculty of Liberal Arts, Thammasat University, Thailand
E-mail: sitthisak.mou@gmail.com

[3]Department of Geosciences and Natural Resource Management, University of Copenhagen, Denmark
E-mail: thbb@ign.ku.dk

**Corresponding Author*

DOI: https://doi.org/10.52939/ijg.v22i3.4873

Abstract

In Thailand, eutrophication remains a critical issue due to high nutrient loading that promotes rapid phytoplankton proliferation. Assessing eutrophication using satellite-derived data is essential, offering a faster, more cost-effective, and less labor-intensive alternative to conventional field-based methods. In this context, the present study evaluates chlorophyll-a estimation algorithms from Sentinel-2 imagery through two approaches: (1) refinement of four previously published algorithms originally developed for temperate or subtropical regions, and (2) development of new region-specific algorithms using multiple linear regression (MLR) and polynomial regression (PO). The results from the first approach indicated that the adjusted chlorophyll-a (Chla) algorithm, validated through 10-fold cross-validation, yielded the best performance among the four, achieving an average R^2 and adjusted R^2 = 0.64, RMSE = 46.25 µg/L, mean bias = -0.58 µg/L, and Index of Agreement (IoA) = 0.88. In the second approach, the PO algorithm exhibited superior predictive accuracy, with R^2 = 0.73, adjusted R^2 = 0.72, RMSE = 39.19 µg/L, mean bias = -4.28 µg/L, and IoA = 0.91. The findings reveal that previously published algorithms developed for temperate or subtropical regions cannot be directly transferred to tropical freshwater lake systems in Thailand, due to differences in ecological dynamics, climate variability and phytoplankton species. The limited performance of unadjusted existing algorithms emphasizes the necessity of locally calibrated algorithms. Therefore, the proposed PO-based empirical algorithm, developed with regional datasets, demonstrates substantial potential for accurate, scalable, and cost-effective chlorophyll-a monitoring.

Keywords: Chlorophyll-a, Eutrophication, Freshwater Bodies, Remote Sensing, Sentinel-2, Water Quality

1. Introduction

Eutrophication is a serious environmental problem commonly occurring in freshwater bodies worldwide. This phenomenon is caused by the excessive accumulation of nutrients such as nitrogen and phosphorus, primarily resulting from human activities including the intensive use of chemical fertilizers in agriculture, wastewater discharge from livestock farms and residential areas, and industrial effluents, which are widely recognized as major sources of nutrient enrichment in freshwater systems worldwide [1][2] and [3]. Nutrient accumulation in aquatic environments promotes excessive growth of phytoplankton and algae, particularly cyanobacteria, microorganisms capable of producing harmful toxins such as microcystins, which pose significant health risks to humans and animals consuming contaminated water [4]. These harmful algal blooms (HABs) not only degrade water quality and limit its usability, but also disrupt ecosystem balance by depleting dissolved oxygen levels, potentially causing mass mortality of aquatic organisms and reducing biodiversity [5] and [6].

In Thailand, eutrophication is observed in several water bodies [7] and [8]. For instance, Bung Sikan and Bung Yai have recorded chlorophyll-a levels exceeding 350 µg/L, representing one of the most severe eutrophication cases in the country and calling for an immediate management response [9] and [10].

Continuous monitoring and tracking of water body conditions are among the key strategies to mitigate the impacts of this problem. However, traditional water sampling and laboratory analysis methods face several limitations such as high costs, resource intensity, and difficulties in covering large areas [1] and [4]. Incorporating remote sensing technology has become an increasingly favored approach in global research. This technology enables data collection over large areas rapidly and accurately, significantly reducing costs and time [5] and [11]. Sentinel-2, a component of the European Union's Copernicus program, is specifically designed for monitoring natural resources and the environment. With spatial resolutions ranging from 10 to 60 meters and spectral coverage across both visible and infrared regions, it is particularly well-suited for observing small-scale inland water bodies and is also suitable for monitoring water bodies in remote and inaccessible areas [10] and [12]. Additionally, Sentinel-2 captures images every five days, allowing continuous tracking of changes in water bodies. Owing to these capabilities, Sentinel-2 satellite data have strong potential for water quality assessment, particularly for evaluating eutrophication status and chlorophyll-a concentrations of phytoplankton in freshwater systems.

In tropical regions, evaluating chlorophyll-a algorithm is a key aspect of assessing the status of water bodies. Chlorophyll-a serves as a crucial indicator of phytoplankton abundance in water bodies, directly reflecting the level of eutrophication [1] and [2]. In these environments, chlorophyll-a concentrations tend to increase rapidly due to high temperatures and high nutrient concentrations [13]. Chlorophyll-a thus serves not only as a proxy for phytoplankton biomass and eutrophication status but also as a key target for algorithm validation. In laboratory and controlled-system studies, chlorophyll-a is commonly extracted in organic solvents (e.g., 90 % acetone for field samples) and quantified spectrophotometrically [14], an approach that informs calibration of satellite-based retrievals. Using Sentinel-2 satellite data, which features high spatial resolution in spectral bands sensitive to chlorophyll-a detection, such as the green and near-infrared bands, is ideal for developing and evaluating chlorophyll-a algorithms in tropical regions [9][12] and [15]. These algorithms enable researchers to predict and monitor changes in chlorophyll-a concentrations effectively, benefiting water resource management in biodiversity-rich freshwater systems.

In Thailand, evaluating chlorophyll-a algorithms in tropical freshwater systems is a growing research interest, as most existing studies focus on temperate or subtropical regions with limited validation under tropical conditions, characterized by high turbidity, diverse phytoplankton, and rapid water quality changes. Sentinel-2-based studies show promising results, particularly in areas like Bung Boraphet and Lam Pao Dam [10], and the use of Google Earth Engine (GEE) helps address field sampling limitations. However, few studies compare multiple algorithms using robust statistical and cross-validation methods, and integrated evaluations across diverse water types (e.g., reservoirs, wetlands, large lakes) with varying optical properties are still lacking. Addressing these gaps is essential to improve algorithm accuracy, transferability, and applicability for tropical freshwater monitoring. Therefore, this study aims to evaluate and develop chlorophyll-a estimation algorithms for tropical freshwater environments in Thailand using Sentinel-2 satellite imagery. Two primary approaches were employed: (1) the implementation and refinement of four previously published algorithms to improve predictive accuracy, and (2) the development of new region-specific empirical algorithms using multiple linear regression (MLR) and polynomial regression (PO) with a10-fold cross-validation approach. These algorithms were designed to enable continuous and scalable predictions of chlorophyll-a concentrations, thereby facilitating more effective assessments of freshwater ecosystem conditions [1] and [16].

2. Methodology

2.1 Study Area

This study covered 50 freshwater bodies across Thailand (Table 1; Figure 1), representing diverse ecological and hydrological conditions. The sites included both anthropogenically influenced systems, affected by agricultural runoff and urban wastewater, and relatively pristine natural reservoirs. Water bodies were classified according to national standards as small ($<2 \times 10^6$ m^3), medium ($2–100 \times 10^6$ m^3), and large ($>100 \times 10^6$ m^3) categories [17]. The southern region was excluded because persistent cloud cover from the southwest and northeast monsoons hinders consistent satellite observation throughout most of the year.

Table 1: Number of water bodies by size class in the study area

Water body size	Number of water bodies	Number of sampling points per water body	Total number of samples
1. Large-sized water bodies	9	9	81
2. Medium-sized water bodies	15	7	105
3. Small-sized water bodies	26	3	78

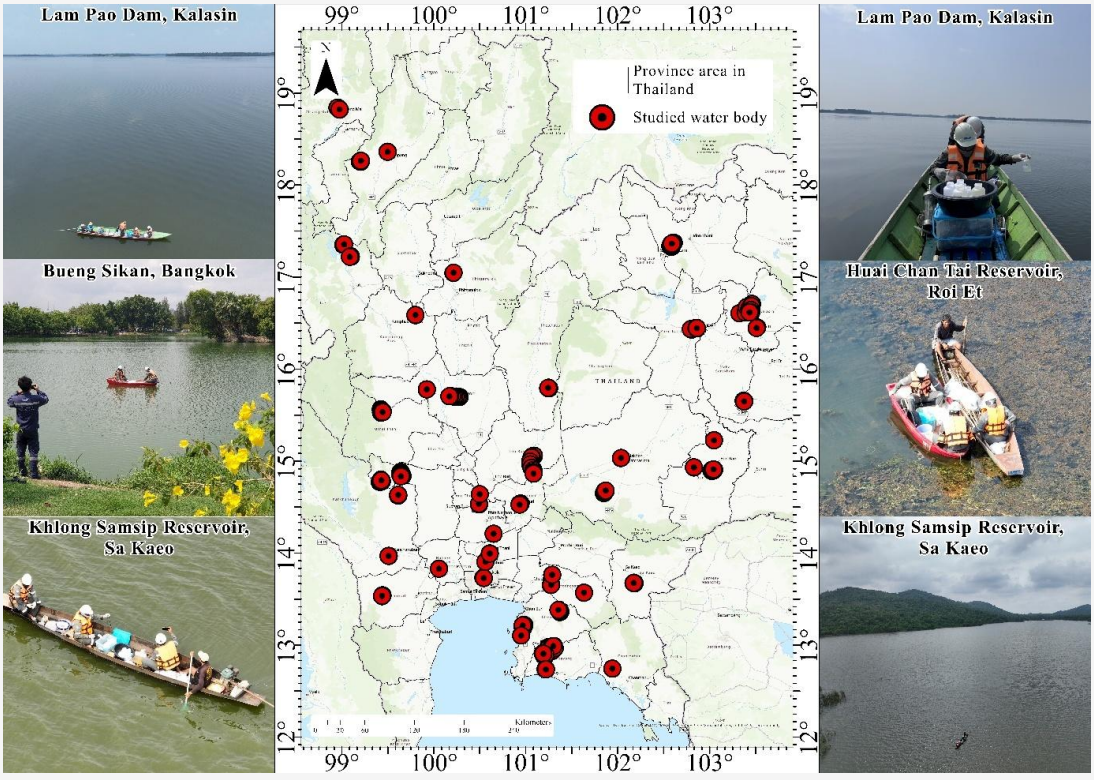

Figure 1: Spatial distribution of the water body sampling locations in Thailand

2.2 Field Data Collection and Water Quality Analysis

Field sampling was carried out during April–May 2024, corresponding to the transition between dry and wet monsoon seasons characterized by high air temperatures (>35 °C) and variable rainfall that stimulate phytoplankton growth. A stratified random sampling approach was applied: all 50 water bodies were categorized by size (small, medium, large), and sampling points were randomly assigned in GIS at proportional densities (3, 7, and 9 sampling points per category). Coordinates were verified in the field using a Garmin GPSMAP 65 Multi-Band unit (horizontal accuracy ±3–5 m, improved to ±1–3 m under open-sky conditions) to ensure proper spatial alignment with Sentinel-2 imagery, allowing a positional tolerance of ±10 m based on 20 m pixel resolution. A total of 264 samples were collected at 1 m depth using 2-L water samplers. This depth minimized surface disturbance but may not fully represent near-surface chlorophyll-a detected by satellites; such depth differences can partly explain discrepancies between in-situ and satellite-derived estimates [4] and [18]. Each site was georeferenced, and field parameters (temperature, pH, dissolved oxygen) were recorded. Chlorophyll-a was extracted with 90 % acetone and analyzed using a dual-beam spectrophotometer (Shimadzu UV-1800).

2.3 Remote Sensing Data and Preprocessing

Satellite imagery from Sentinel-2 used in this study was obtained from the Copernicus Open Access Hub. Acquisition dates were aligned with field sampling (April–May 2024), ensuring temporal consistency between in-situ observations and satellite data. The selected Sentinel-2 Level-1C images were atmospherically corrected to Level-2A surface reflectance using Sen2Cor processor (version 2.10), which applies a radiative transfer-based approach to separate atmospheric and surface contributions, to minimize atmospheric effects [12] and [19]. Default processing settings were applied, including the

continental aerosol model and standard ozone and water-vapor profiles. Sen2Cor was selected as it is the European Space Agency (ESA) standard atmospheric correction processor and widely used for inland and coastal water applications [11] and [20]. The top-of-atmosphere reflectance was calculated as shown in Equation 1.

$$L_{TOA} = L_{Atmosphere} + L_{surface}$$

Equation 1

Where: L_{TOA} is top-of-atmosphere reflectance, $L_{Surface}$ is surface reflectance, and $L_{Atmosphere}$ is atmospheric contribution.

Sentinel-2 MSI provides multispectral bands at different spatial resolutions (10–60 m). Table 2 summarizes the key bands used for chlorophyll-a retrieval, including their wavelength ranges, spatial resolutions, and established applications [12][15] and [21]. After atmospheric correction, all bands were resampled to a uniform 20 m resolution using bilinear interpolation, which provides an appropriate balance between spatial precision and consistency with the field sampling scale.

To ensure data quality, Sentinel-2 scenes with cloud cover greater than 10%, derived from scene-level cloud metadata, were excluded. This scene-level cloud screening follows the conceptual basis of the Sentinel-2 Cloud Masking Algorithm (S2-CMA), which utilizes cirrus (Band 10), water vapor absorption (Band 9), and scene brightness characterize cloud contamination, without explicitly implementing pixel-wise cloud probability estimation. Non-water areas (e.g., forest, urban, bare land) were masked using the ESA WorldCover 10 m V2.0 dataset (ESA, 2020). Remaining pixels were refined with the Normalized Difference Water Index (NDWI) computed from surface reflectance. The *NDWI* was calculated as shown in Equation 2.

$$NDWI = \frac{B3 - B8}{B3 + B8}$$

Equation 2

Where: *B3* (560 nm) is the green band and *B8* (842 nm) is the near-infrared band. Pixels with NDWI > 0.2 were classified as water, reducing misclassification in turbid or vegetated zones [22] and [23].

2.4 Chlorophyll-a Estimation

Two approaches to develop algorithms for estimating chlorophyll-a concentrations were applied. The first approach involves improving previously published algorithms, as their preliminary application to freshwater systems in Thailand resulted in limited predictive accuracy likely due to differences in bio-optical conditions between tropical and temperate or subtropical regions. This limitation highlights the need for algorithm refinement and local recalibration. The second approach involves the development of new region-specific algorithms through MLR and PO. Data obtained from both approaches were then compared to assess their accuracy for selecting algorithm that provides the most reliable chlorophyll-a estimation for Thailand. Figure 2 illustrates the overall workflow for both approaches, from initial data partitioning to final algorithm selection and application.

2.5 Using Previously Published Chlorophyll-a Algorithms

Following atmospheric correction and image preprocessing, four published chlorophyll-a algorithms were applied to evaluate the performance of satellite-derived water quality estimates against in-situ measurements (Table 3). This preliminary assessment identified formulas that performed relatively better than others when compared with field observations; however, their predictive accuracy remained limited, necessitating further algorithm refinement.

Table 2: Sentinel-2 MSI bands relevant to chlorophyll-a estimation

Band	Central wavelength (nm)	Resolution (m)	Application	References
B2 (Blue)	490	10	Water absorption, suspended matter	[12]
B3 (Green)	560	10	Chlorophyll reflectance peak	[24]
B4 (Red)	665	10	Chl-a absorption	[21]
B5, B6, B7 (Red-edge)	705–783	20	Chlorophyll sensitivity	[15]
B8, B8A (NIR)	842–865	10/20	Algal bloom detection	[16]
B11, B12 (SWIR)	1610/2190	20	Turbidity, atmospheric correction	[25]

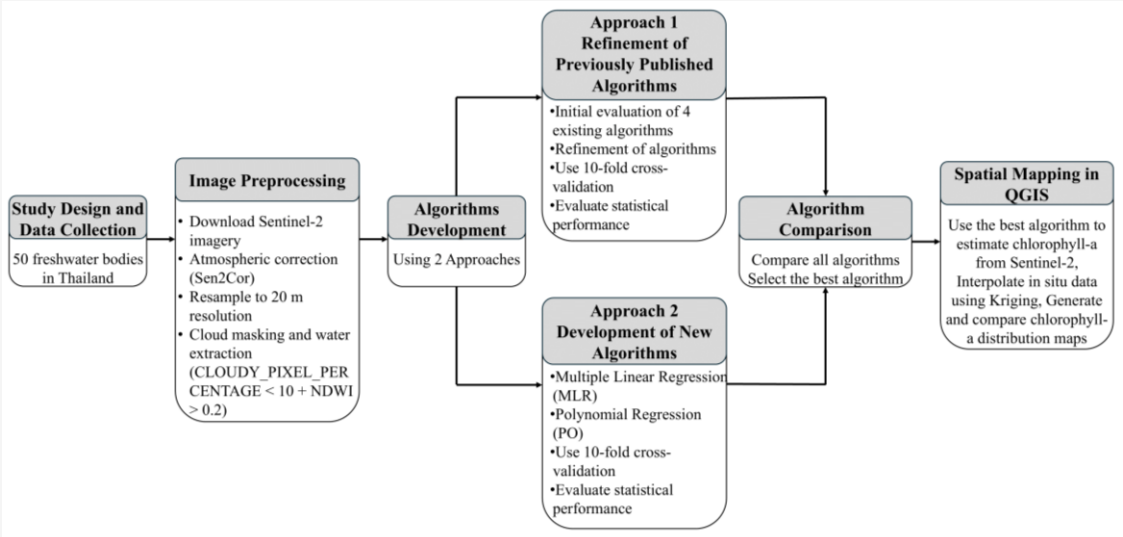

Figure 2: Workflow for chlorophyll-a algorithm development: Approach 1 refines four previously published algorithms via iterative band addition, coefficient re-estimation, and cross-validation; Approach 2 builds new region-specific empirical algorithms (MLR and PO) through systematic predictor selection and 10-fold CV

Table 3: Previously published chlorophyll-a algorithms used for chlorophyll-a concentration estimation

Name	Algorithm	References
Chla	$Chla = (B5 + B6) / B4$	[15]
C_{chla}	$C_{chla} = 10^{0.0844 - 1.968R + 9.1257R^2 + 61.573R^3 + 86.808R^4}$	[16]
Chl_{NN}	$Chl_{NN} = 21a_{pig}^{1.04}$	[26]
Chl-a	$Chl\_a = 14.039 + 86.115NDCI + 194.325NDCI^2$	[27]

According to Table 3, the parameters used in the chlorophyll-a algorithms are defined in Equations 3 to 5:

$$R = \log_{10}\left(\max\times\frac{\left(Rrs_{443}\times Rrs_{531}\right)}{Rrs_{490}}\right) \quad \text{Equation 3}$$

Where: Rrs_x is the wavelength of WorldView-3 bands

$$a_{pig} = CDOM = \frac{B3 - B1}{B3 + B1} \quad \text{Equation 4}$$

Where: B is Band of Sentinel-2 satellite

$$NDCI = \frac{B5 - B4}{B5 + B4} \quad \text{Equation 5}$$

Where: NDCI is Normalized Difference Chlorophyll Index

The algorithm performance was quantitatively evaluated using five statistical indicators: coefficient of determination (R^2; Equation 6), root mean square error (*RMSE*; Equation 7), mean bias (Equation 8), index of agreement (*IoA*; Equation 9), and adjusted R^2 (R^2_{adj}; Equation 10). These metrics provided a comprehensive measure of accuracy and reliability relative to field-based chlorophyll-a data.

$$R^2 = 1 - \frac{\sum_{i=1}^{n}\left(y_i - \hat{y}_i\right)^2}{\sum_{i=1}^{n}\left(y_i - \bar{y}_i\right)^2} \quad \text{Equation 6}$$

$$RMSE = \sqrt{\frac{1}{n}\sum_{i=1}^{n}\left(y_i - \hat{y}_i\right)^2} \quad \text{Equation 7}$$

$$Mean\ bias = \frac{1}{n}\sum_{i=1}^{n}\left(y_i - \hat{y}_i\right) \quad \text{Equation 8}$$

$$IoA = 1 - \frac{\sum_{i=1}^{n}\left(y_i - \hat{y}_i\right)^2}{\sum_{i=1}^{n}\left(\left|y_i - \bar{y}\right| + \left|\hat{y}_i - \bar{y}\right|\right)^2}$$

Equation 9

$$R^2_{adj} = 1 - \left(\frac{\left(1 - R^2\right)(n-1)}{n-k-1}\right)$$

Equation 10

Where: R^2 is the coefficient of determination, *RMSE* is the root mean square error, mean bias is the average error, *IoA* is the index of agreement, R^2_{adj} is the adjusted coefficient of determination, n is the number of samples and k is the number of predictors, $\hat{y}_i$ and y_i are the predicted and observed chlorophyll-a values, respectively, and $\bar{y}_i$ is the mean of the observed values.

Based on this evaluation, the most accurate algorithms were selected for subsequent refinement. Additional Sentinel-2 spectral bands (e.g., red-edge, SWIR) were iteratively incorporated into each base algorithm, and coefficients were re-estimated using ordinary least squares with the full calibration dataset. Each modified algorithm was validated using 10-fold cross-validation. Predictor terms that did not significantly improve adjusted R^2 were removed. This iterative procedure was repeated until no further improvement was achieved, ensuring that the final "adjusted" algorithms achieved an optimal balance between explanatory power and generalization, minimizing overfitting while enhancing performance for Sentinel-2-based chlorophyll-a retrieval in tropical freshwater systems.

2.6 Using New Region-Specific Algorithms through the 10-Fold Cross-Validation Technique

Because the previously published algorithms (Approach 1) showed limited accuracy when applied to the study area, a second approach was implemented to develop new region-specific algorithms using two regression techniques: Multiple Linear Regression (MLR) and Polynomial Regression (PO). Both approaches incorporated additional explanatory variables derived from Sentinel-2 spectral bands and indices. A stepwise selection procedure was used to identify the optimal combination of predictors. At each iteration, variables were added or removed based on their statistical contribution as measured by adjusted R^2, and the process continued until no further improvement was achieved. This approach integrates the advantages of both forward and backward selection, resulting in a parsimonious yet informative algorithm structure.

For the MLR approach, chlorophyll-a concentration was algorithm as a linear combination of selected predictor variables, as expressed in Equation (11). The performance of each algorithm was then validated through 10-fold cross-validation. Sentinel-2 MSI was selected for its high spatial resolution and broad spectral coverage, suitable for monitoring optically complex tropical waters [12] and [22]. These regression techniques have demonstrated strong predictive capacity for algorithm spectral–chlorophyll-a relationships in tropical freshwater systems [5][16] and [28]. The MLR was calculated as shown in Equation 11.

$$Chlorophyll - a = \beta_0 + \beta_1 X_1 + \beta_2 X_2 + ... + \beta_n X_n + \varepsilon$$

Equation 11

Where: *Chlorophyll-a* is the concentration (dependent variable); β_0 is the intercept; $\beta_1, \beta_2, \ldots, \beta_n$ are the regression coefficients; X_1, X_2, …, X_n represent Sentinel-2 reflectance bands (e.g., B2, B3, B4, B5, B8) and derived spectral indices (e.g., NDCI), selected through stepwise regression; and ε is the error term.

PO was employed when non-linear relationships were detected between predictors and chlorophyll-a concentrations. The PO was calculated as shown in Equation 12.

$$Chlorophyll - a = a\sum_{i=1}^{n} b_i X_i + \sum_{i=1}^{n} c_i X_i^2 + \sum_{i=1}^{n-1}\sum_{j=i+1}^{n} d_{ij} X_i X_j + \varepsilon$$

Equation 12

Where: *Chlorophyll-a* is the chlorophyll-a concentration (dependent variable); a is the intercept; b_i and c_i are coefficients of the linear and quadratic terms of the independent variables, respectively; d_{ij} represents the interaction coefficients between independent variables X_i and X_j; X_i and X_j denotes the independent variables; and ε is the error term.

2.7 The 10-Fold Cross-Validation between Two Approaches

To ensure a robust comparison of predictive performance, all algorithms were validated using 10-fold cross-validation. The dataset was randomly divided into ten equal subsets; in each iteration, nine subsets were used for algorithm training and one for validation, rotating until each subset had served once as the validation set. Algorithm parameters were

estimated using ordinary least squares (OLS), which minimizes the sum of squared residuals. For each fold, the following performance metrics were calculated: R^2, *RMSE*, mean bias, *IoA*, and R^2_{adj}. Average values across all folds were then derived to represent overall algorithm accuracy. This validation strategy reduces overfitting, improves algorithm generalization, and ensures the selection of a stable and reliable algorithm for practical freshwater quality monitoring. All analyses were performed using Microsoft Excel and Google Colaboratory.

2.8 Spatial Mapping of Chlorophyll-a Distribution from Field Measurements and Sentinel-2

Data from both approaches were compared to identify the most accurate algorithm for chlorophyll-a estimation in Thailand. The selected algorithm was then applied to generate spatial chlorophyll-a distribution maps from Sentinel-2 imagery using QGIS, enabling evaluation of its spatial performance. Field-derived chlorophyll-a data, stored as point vectors, were analyzed alongside satellite-based estimates derived from the optimal algorithm. Both datasets were integrated in QGIS to produce comparable spatial layers. Surface interpolation of field measurements was performed using the Ordinary Kriging technique, which is suitable for spatially correlated environmental data [9]. Sampling coordinates were georeferenced using GPS, and the interpolated chlorophyll-a surfaces were expressed in µg/L. Satellite-derived maps were clipped to the study boundaries and classified using identical color scales and concentration units. Direct comparison between the two map types allowed quantitative assessment of the algorithm's accuracy and its ability to reproduce observed spatial variability.

3. Results

3.1 Performances of Previously Published Chlorophyll-a Algorithms

A quantitative evaluation of four previously published chlorophyll-a retrieval algorithms (C_{chla} [16], Chl_{NN} [26], *Chla* [15], and *Chl-a* [27]) was conducted using in situ chlorophyll-a measurements as ground truth. The results, summarized in Table 4, indicate substantial variability in predictive performance across the algorithms. Among them, the *Chl-a* [27] algorithm exhibited relatively better predictive performance, achieving the highest R^2 (0.12), the lowest *RMSE* (72.76 µg/L), the lowest mean bias (-34.96 µg/L), and the highest *IoA* (0.53). These metrics collectively suggest a reasonable correspondence between the modeled and observed chlorophyll-a concentrations. Conversely, the C_{chla} [16] and *Chla* [15] algorithms yielded lower predictive performance, with strongly negative R^2 values (-0.81 and -0.77, respectively), elevated *RMSE* (>100 µg/L), and large negative biases (-69.72 and -68.64 µg/L), indicative of systematic underestimation. The Chl_{NN} [26] algorithm performed marginally better but still demonstrated limited predictive capacity (R^2 = -0.49, *RMSE* = 94.29 µg/L, *IoA* = 0.38). Despite the generally low or negative R^2 values, likely attributable to the nonlinearity and variability inherent in optically complex inland waters [18] and [21], the *Chl-a* [27] algorithm stands out as the most robust among the tested algorithms. Its relative accuracy supports its selection as a baseline algorithm for subsequent algorithm tuning and regional recalibration under the specific bio-optical conditions of the study area.

Figure 3 visually reinforces the statistical evaluation summarized in Table 3 by depicting scatter plots of in situ chlorophyll-a concentrations against estimates from four previously published algorithms, (C_{chla} [16], Chl_{NN} [26], *Chla* [15], and *Chl-a* [27]), each accompanied by fitted regression lines and shaded confidence intervals. Among the algorithms, the *Chl-a* [27] algorithm, identified as the best performing in terms of R^2 (0.12), *RMSE* (72.76 µg/L), mean bias (-34.96 µg/L), and *IoA* (0.53), displays a distinct positive linear trend with tightly clustered data points and a narrow uncertainty band, reflecting strong predictive agreement and stability under local optical conditions. The *Chla* [15] algorithm, although quantitatively less accurate (R^2 = -0.77), still shows a moderately positive slope and acceptable data dispersion, indicating its potential to capture variability despite systematic underestimation. In contrast, both C_{chla} [16] and Chl_{NN} [26] demonstrate weak to negative associations with observed values. The Chl_{NN} [26] algorithm, in particular, exhibits a downward-sloping trend line and wide uncertainty bounds, highlighting limited generalization and low reliability. Collectively, the visual and statistical evidence supports the *Chl-a* [27] algorithm as the most appropriate candidate for further refinement and site-specific calibration, while also indicating that the other algorithms, especially C_{chla} [16] and Chl_{NN} [26], require substantial recalibration or structural adjustment. Among the evaluated algorithms, the *Chl-a* [27] showed the highest correlation with field data, with $r = 0.76$ ($p < 0.01$), where r denotes the Pearson correlation coefficient, followed by *Chla* [15] algorithm, which yielded $r = 0.71$ ($p < 0.01$).

Table 4: Performance metrics of previously published chlorophyll-a algorithms compared to in situ observation

Algorithm	R^2	*RMSE* (µg/L)	Mean Bias (µg/L)	*IoA*	Min (µg/L)	Max (µg/L)	Mean (mean±SD; µg/L)
C_{chla} [16]	-0.81	104.15	-69.72	0.41	1.08	2.59	1.43±0.30
Chl_{NN} [26]	-0.49	94.29	-51.93	0.38	9.63	26.15	19.23±3.62
Chla [15]	-0.77	103.04	-68.64	0.41	0.99	5.21	2.51±0.73
Chl-a [27]	0.12	72.76	-34.96	0.53	9.73	92.84	36.19±19.74
Chlorophyll-a in situ observation					1.00	357.62	71.16±78.15

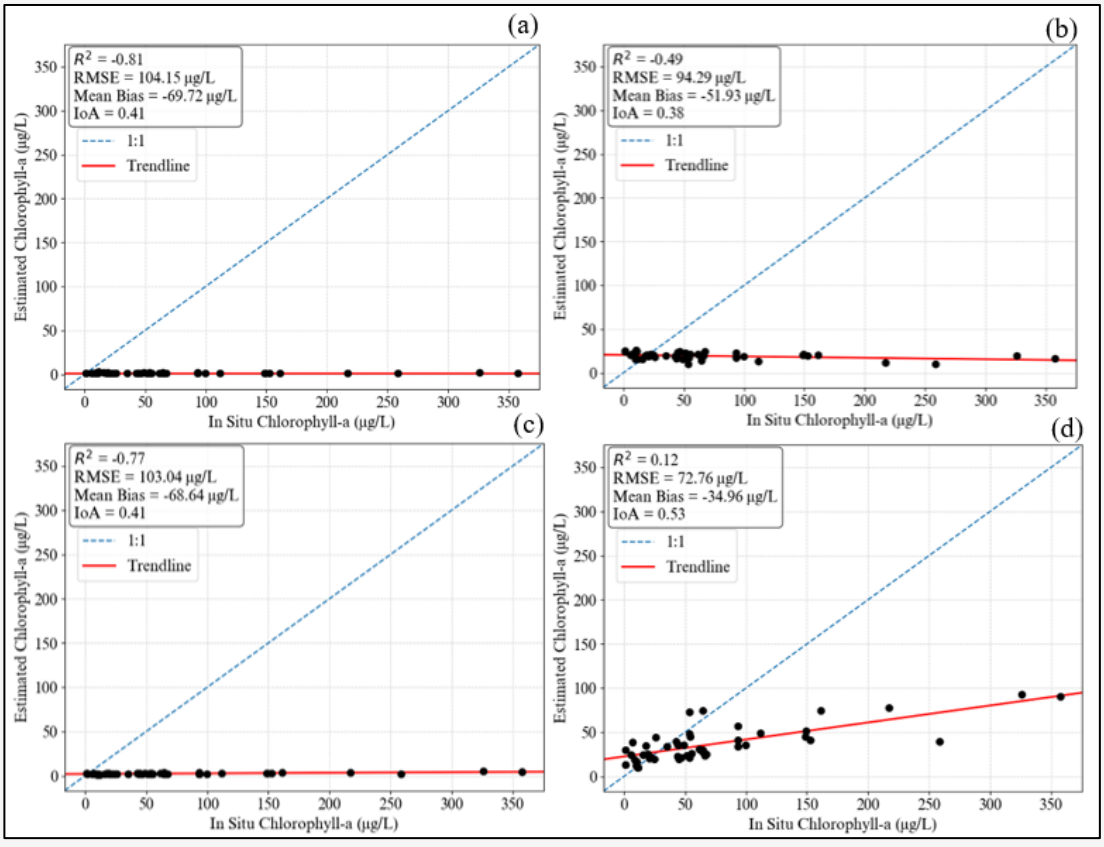

Figure 3: Comparison of satellite-derived chlorophyll-a estimates from previously published algorithms: (a): C_{chla} [16], (b): Chl_{NN} [26], (c): *Chla* [15] and (d): *Chl-a* [27]) against in situ chlorophyll-a measurements

Table 5: Performance metrics and summary statistics of adjusted chlorophyll-a estimation algorithms

Algorithm	R^2 (mean±SD)	R^2_{adj} (mean±SD)	*RMSE* (mean±SD); (µg/L)	Mean Bias (mean±SD); (µg/L)	*IoA* (mean±SD)	Min (µg/L)	Max (µg/L)	Mean (mean±SD); (µg/L)
Adjusted Chla algorithm ($Chla_{adj}$)	0.64±0.01	0.64±0.01	46.25±0.69	-0.58±2.75	0.88±0.01	0.00	290.99	69.64±61.00
Adjusted Chl-a algorithm ($Chl\text{-}a_{adj}$)	0.62±0.01	0.61±0.01	47.55±0.36	-0.51±3.13	0.87±0.01	13.21	287.71	70.57±59.41
Chlorophyll-a in situ observation						1.00	357.62	71.16±78.15

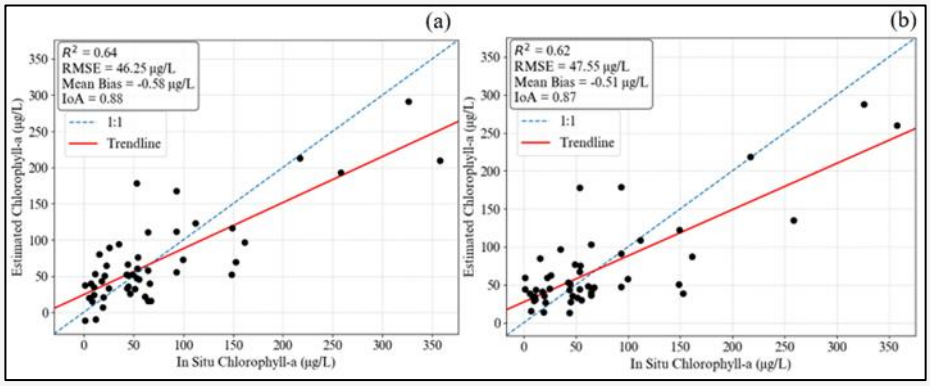

Figure 4: Comparison of satellite-derived chlorophyll-a estimates after refinement with in situ chlorophyll-a measurements: (a) Adjusted *Chla* algorithm, and (b) Adjusted *Chl-a* algorithm

These results indicate that both algorithms have strong potential for accurately estimating chlorophyll-a concentrations from satellite data in optically complex freshwater environments. As such, they are considered suitable candidates for further algorithm refinement. We enhanced the performance of the chlorophyll-a algorithms (*Chla* [15] and *Chl-a* [27]) by incorporating additional spectral bands from Sentinel-2 satellite imagery. Hereafter, the refined versions of the previously published *Chla* [15] and *Chl-a* [27] algorithms are referred to as the adjusted *Chla* ($Chla_{adj}$) and the adjusted *Chl-a* ($Chl\text{-}a_{adj}$) algorithms, respectively. Table 5 and Figure 4 presents the performance statistics of the refined chlorophyll-a estimation algorithms, both with and without 10-fold cross-validation, in comparison with in situ field observations. The $Chla_{adj}$ algorithm without cross-validation achieved an R^2 of 0.64, an R^2_{adj} of 0.64, an *RMSE* of 46.25 µg/L, a mean bias of -0.58 µg/L, and *IoA* of 0.88. These metrics indicate a satisfactory predictive performance. When evaluated using 10-fold cross-validation, the $Chla_{adj}$ algorithm demonstrated comparable accuracy, with identical R^2 and R^2_{adj} values of 0.64 and 0.64 in average, respectively. The *RMSE* slightly increased to 46.25 µg/L in average, and the mean bias shifted to -0.58 µg/L in average. The *IoA* remained unchanged at 0.88 in average. The mean ± standard deviation of predicted chlorophyll-a concentrations for this algorithm was 69.64±61.00 µg/L.

The $Chl\text{-}a_{adj}$ algorithm without cross-validation showed marginally lower performance, with R^2 and R^2_{adj} values of 0.62 and 0.61, respectively. The *RMSE* was 47.55, the mean bias was -0.51, and the *IoA* was 0.87. The $Chl\text{-}a_{adj}$ yielded R^2 = 0.62 and *RMSE* = 47.55 µg/L based on 10-fold cross-validation. Results without cross-validation are also reported for comparison in Table 5, but unless otherwise specified, the discussion refers to cross-validated results, yielded consistent results, with R^2 and R^2_{adj} of 0.62 and 0.61, respectively, a slightly increased *RMSE* of 47.55 µg/L in average, and a mean bias of -0.51 µg/L in average. The *IoA* remained at 0.87 in average, reflecting a stable level of algorithm performance. The $Chla_{adj}$ and $Chl\text{-}a_{adj}$ were calculated according to Equations 13 and 14.

$$Chla_{adj} = 25.334 - 0.145B2 + 0.197B6 + 0.496B7 - 0.650B8A + 0.079B12 \quad \text{Equation 13}$$

$$Chl\text{-}a_{adj} = 30.634 - 321.121NDCI + 2.165(NDCI \times B7) - 1.862(NDCI \times B8A) \quad \text{Equation 14}$$

Where: *B2* is the Blue band (490 nm), *B6* is the Vegetation Red-Edge band 2 (740 nm), *B7* is the Vegetation Red-Edge band 3 (783 nm), *B8A* is the Narrow Near-Infrared (NIR) band (865 nm), and *B12* is the Short-Wave Infrared (SWIR 2) band (2190 nm).

The recalibration of previously published algorithms highlights the strong influence of local optical properties in tropical waters. Variations in turbidity, dissolved organic matter, and phytoplankton composition alter reflectance–chlorophyll relationships. Therefore, while previously published algorithms provide useful baselines, site-specific calibration is essential for accurate application in tropical freshwater ecosystems.

3.2 Performances of New Region-Specific Algorithms Developed Using Multiple Linear Regression and Polynomial Regression

The results of a comparative evaluation of statistical metrics between in situ chlorophyll-a measurements and algorithm-derived estimates, using two algorithms, MLR and PO, validated through 10-fold cross-validation, are presented in Table 6 and Figure

5. Hereafter, the new region-specific algorithms based on multiple linear regression and polynomial regression are referred to as the *Chl-a* Linear algorithm (*Chl-a*$_L$) and *Chl-a* Polynomial algorithm (*Chl-a*$_P$), respectively. The *Chl-a* Linear algorithm achieved an R^2 of 0.66 and R^2_{adj} of 0.66 in average, indicating moderate predictive ability. *RMSE* was 44.76 µg/L in average, and the mean bias was relatively low at -0.29 µg/L in average. The *IoA* was 0.89 in average, reflecting good agreement between algorithm predictions and field observations. The predicted chlorophyll-a concentrations ranged from 5.01 – 320.17 µg/L, with a mean ± standard deviation of 70.86±63.12 µg/L. In contrast, the *Chl-a*$_p$ algorithm showed superior performance across all key metrics. It yielded a higher R^2 of 0.73 and R^2_{adj} of 0.72 in average, indicating strong predictive accuracy. The *RMSE* was substantially lower at 39.19 µg/L in average, although the mean bias increased to -4.28 µg/L in average. The *IoA* improved to 0.91 in average, suggesting a high degree of alignment between the algorithm output and observed data. The chlorophyll-a values predicted by the polynomial algorithm ranged between 0.82 – 381.80 µg/L, with a mean ± standard deviation of 61.25±51.21 µg/L. The *Chl-a*$_L$ and *Chl-a*$_P$ were calculated according to Equations 15 and 16.

$$Chl\text{-}a_L = 0.481 + 0.706chla\_3af + 0.449chla\_4af - 68769NDCI \quad \text{Equation 15}$$

$$Chl\text{-}a_P = -0.579 + 0.991chla\_3af - 0.842chla\_4af + 379.939NDCI + 0.025chla\_3af^2 - 0.050(chla\_3af \times chla\_4af) - 2.194(chla\_3af \times NDCI) + 0.029chla\_4af^2 - 1.737(chla\_4af \times NDCI) - 1007.816NDCI^2 \quad \text{Equation 16}$$

Where: *chla_3af* is *Chla*$_{adj}$ algorithm, *chla_4af* is *Chl-a*$_{adj}$ algorithm, *B4* is the red band (665 nm), *B5* is the visible and near infrared band (705 nm).

Overall, the results indicate that the polynomial regression algorithm significantly outperformed the linear algorithm in estimating chlorophyll-a concentrations. This is particularly evident in its higher R^2_{adj} and lower *RMSE* values, highlighting its greater reliability and suitability for practical applications in water quality monitoring.

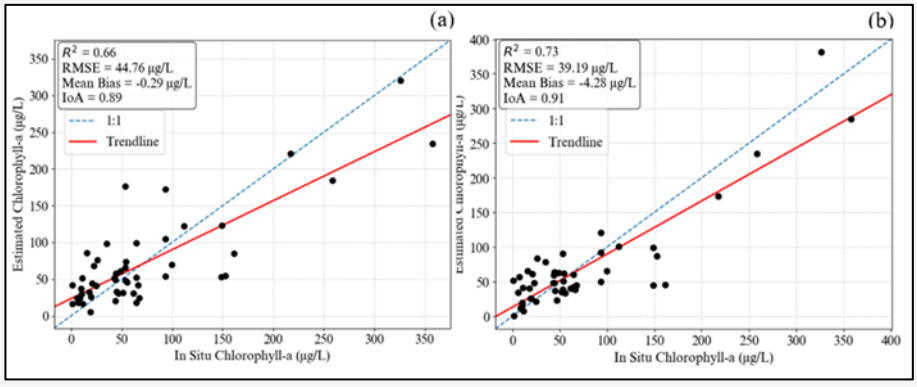

Figure 5: Performance comparison of new region-specific chlorophyll-a algorithms using 10-fold cross-validation: (a) the *Chl-a* Linear algorithm and (b) the *Chl-a* Polynomial algorithm.

Table 6: Performance metrics and summary statistics of new region-specific chlorophyll-a algorithms

Algorithm	R^2 (mean±SD)	R^2_{adj} (mean± SD)	*RMSE* (mean±SD; µg/L)	Mean Bias (mean±SD; µg/L)	*IoA* (mean±SD)	Min (µg/L)	Max (µg/L)	Mean (mean±SD; µg/L)
Chl-a Linear (this study) algorithm	0.66±0.01	0.66±0.00	44.76±0.31	-0.29±3.12	0.89±0.01	5.01	320.17	70.86±63.12
Chl-a Polynomial (this study) algorithm	0.73±0.05	0.72±0.05	39.19±3.43	-4.28±5.22	0.91±0.03	0.82	381.80	61.25±51.21
Chlorophyll-a in situ observation						1	357.62	71.16±78.15

Based on the comparison between two approaches (1) refinement of four previously published algorithms and (2) development of new region-specific algorithms using MLR and PO, the newly developed *Chl-a*$_p$ algorithm achieved the highest predictive accuracy. It outperformed both the refined previously published algorithms and the MLR-based algorithm.

3.3 Spatial Mapping of chlorophyll-a Distribution from Feld Measurements and Sentinel-2 Imagery

For Thap Salao Dam (large-sized water body), Huai Luang Dam (medium-sized water body), and Suan Lumphini (small-sized water body) (Figure 6), chlorophyll-a maps derived from in-situ Kriging and Sentinel-2 *Chl-a*$_p$ algorithm showed generally similar spatial trends, although noticeable local discrepancies were observed. Kriging maps exhibited smoother gradients influenced by sampling density, whereas Sentinel-2 products revealed finer, patchier variations linked to surface reflectance heterogeneity. Peak values from satellite-derived estimates were slightly higher, particularly along the dam crest in the large water body. This discrepancy may be attributed to the absence of in situ sampling points in that area, reflecting a limitation of the present study. For the medium-sized and small-sized water bodies, the color patterns were more consistent, likely because the sampling points provided better spatial coverage across these areas. Nevertheless, some partial data gaps remained in the satellite-derived maps due to cloud cover, shadow effects, and vegetation interference.

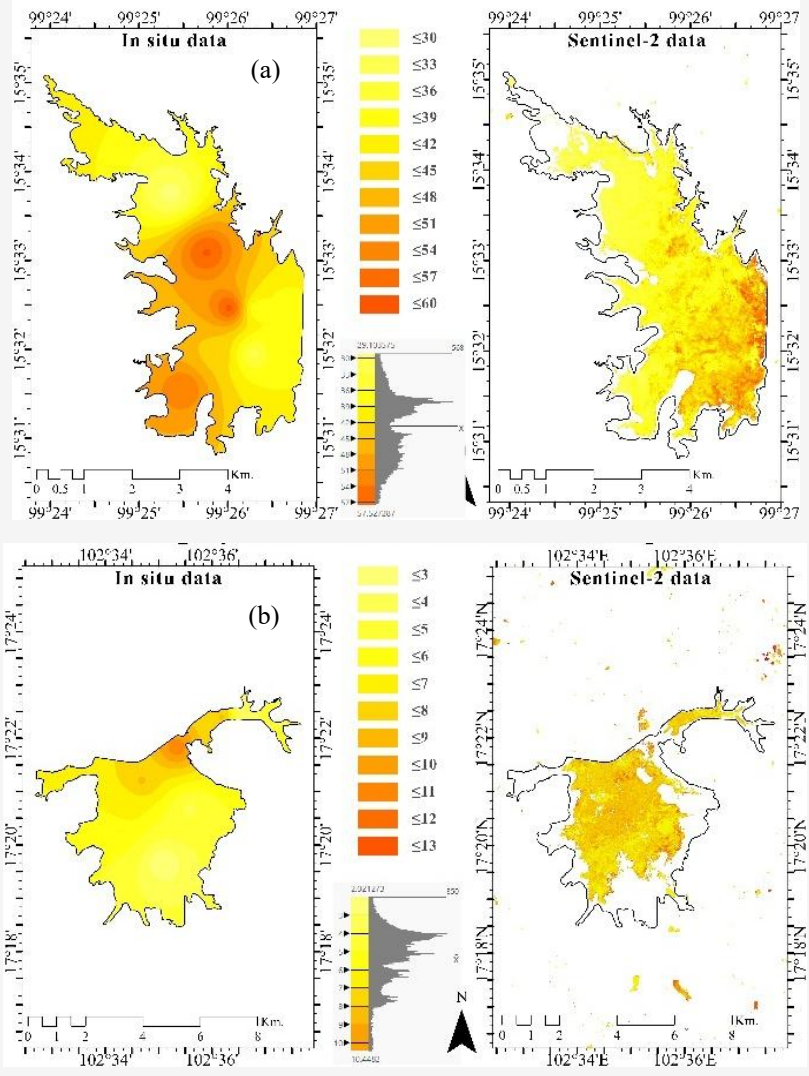

Figure 6: Comparison of chlorophyll-a distributions derived from in situ Kriging and Sentinel-2 Chl-a Polynomial estimates: (a) Thap Salao Dam (large-sized water body), (b) Huai Luang Dam (medium -sized water body) (Continue next page)

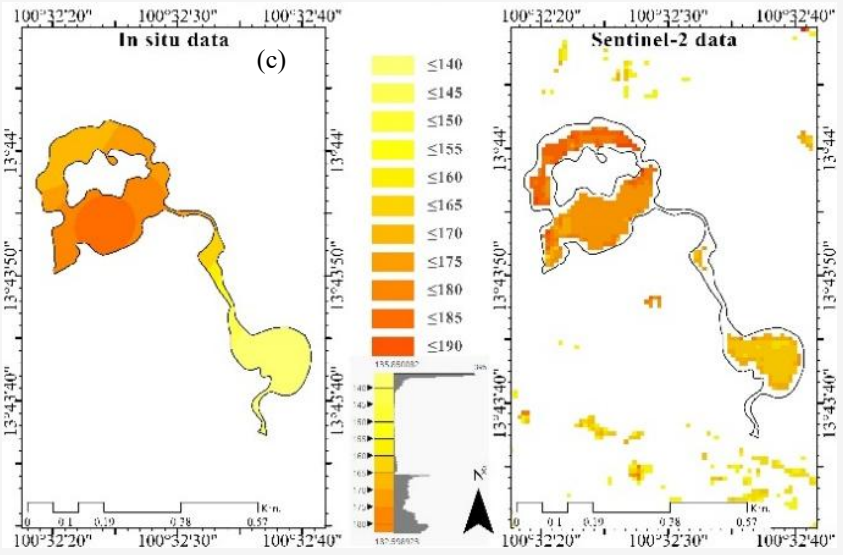

Figure 6: Comparison of chlorophyll-a distributions derived from in situ Kriging and Sentinel-2 Chl-a Polynomial estimates: (c) Suan Lumphini (small-sized water body) (Continue from previous page)

4. Discussion

4.1 Comparison of Chlorophyll-a Estimation using Previously Published Algorithms and New Region-Specific Algorithms

The comparison between previously published algorithms and the new region-specific algorithms revealed notable differences in predictive performance, largely reflecting the underlying methodology and adaptability of each approach. Among the four previously published algorithms, the *Chl-a* [15] algorithm based on the Normalized Difference Chlorophyll Index (NDCI) and near-infrared bands demonstrated the highest accuracy, consistent with [21], who emphasized the effectiveness of NDCI in detecting chlorophyll-a in turbid waters. However, the locally calibrated *Chla* algorithm further improved performance by capturing nonlinear relationships through PO. Nevertheless, the new region-specific *Chl-a*$_P$ exhibited the best overall accuracy, reflecting its ability to integrate multiple predictors, represent nonlinear spectral biophysical relationships, and adapt to the optical complexity of tropical freshwater systems.

Compared with previous research, our polynomial algorithm outperformed the MLR-based approach reported by [29], which achieved an R^2 of 0.65 and *RMSE* of 17 mg/m³, while our algorithm attained higher accuracy. Similarly, [30] obtained an R^2 of 0.85 using machine learning, but with greater algorithm complexity and higher data requirements. In contrast, our polynomial algorithm provides comparable accuracy with simpler implementation, consistent with [31], who reported that PO can achieve high performance without deep-learning frameworks or complex calibration procedures.

4.2 Spatial Application of the Optimized Chlorophyll-a Algorithm

Our new region-specific *Chl-a*$_P$ algorithm achieved the highest *IoA* and demonstrated general consistency with in-situ observations, indicating numerical stability and operational reliability. Its predicted mean chlorophyll-a concentration was comparable to measured values and captured the main spatial variability observed in the field, although localized discrepancies remained. High chlorophyll-a concentrations were accurately captured in eutrophic zones, particularly at sites 30–50. The spatial distribution patterns derived from Sentinel-2 imagery corresponded well with Kriging-based field maps, highlighting the algorithm's applicability for routine monitoring. Water surface area may also influence spatial chlorophyll-a distribution. Larger reservoirs generally promote horizontal mixing and longer residence times, dispersing phytoplankton more evenly. Conversely, small ponds and narrow embayments tend to retain nutrients and algal biomass due to limited circulation, resulting in locally elevated chlorophyll-a levels. This relationship suggests that water surface area indirectly regulates chlorophyll-a through its control of hydrodynamic and nutrient conditions, consistent with observations in other tropical freshwater systems [9].

Differences between Kriging- and satellite-based maps can be attributed to data resolution and sampling constraints. Kriging tends to produce smoother gradients influenced by sampling density,

whereas satellite-derived maps captured fine-scale heterogeneity but sometimes overestimated absolute concentrations. Additional sources of discrepancy include uneven shoreline sampling [32], which could be mitigated by increasing the number and spatial coverage of in situ sampling points to improve the agreement between field-based interpolations and satellite-derived estimates, as well as potential reflectance bias from turbid or shallow areas [23] and [33], and atmospheric correction uncertainties [34]. Minor temporal mismatches between field and satellite acquisition may also affect results [35]. Integrating both datasets using regression Kriging could exploit the high spatial resolution of Sentinel-2 while maintaining field-based accuracy [36].

4.3 Challenges and Future Research Directions

Despite the strong agreement between the new region-specific *Chl-a*$_P$ algorithm and in-situ observations, several challenges remain for its long-term application, particularly in further improving algorithm accuracy and robustness. The reliance on Sentinel-2 imagery limits temporal coverage due to its five-day revisit cycle, potentially constraining near-real-time monitoring during bloom events. Another limitation is the depth mismatch between 1 m field samples and surface reflectance, which may partly explain underestimations or overestimations in satellite retrievals [4] and [18].

In tropical freshwater systems, ecological dynamics and climate variability strongly influence phytoplankton assemblages, pigment composition, and optical water properties, which directly affect the performance of satellite-based chlorophyll-a detection algorithms [21] and [23]. Seasonal variations in temperature and precipitation regulate phytoplankton growth rates and species dominance, while rainfall-driven runoff alters nutrient inputs, turbidity, and colored dissolved organic matter (CDOM), thereby modifying the spectral reflectance–chlorophyll-a relationship [33] and [34]. During wet periods, elevated suspended sediments and CDOM can partially mask chlorophyll-a signals, increasing uncertainty in satellite-derived estimates [35]. These dynamic environmental conditions vary across regions and climatic zones and help explain the reduced transferability of chlorophyll-a algorithms developed in temperate or subtropical regions when applied to optically complex tropical waters, emphasizing the need for region-specific calibration and validation [16] and [21]. Expanding region-specific datasets and applying hyperspectral imagery could also refine predictive capabilities.

While MLR and PO approaches yielded reliable results, they remain limited in representing complex nonlinear interactions within heterogeneous tropical systems. Machine learning techniques, such as Random Forest or Artificial Neural Networks, have demonstrated superior flexibility and may further enhance accuracy in turbid or CDOM-rich waters [16][21] and [26]. Moreover, integrating geospatial and AI-based monitoring systems could facilitate near real-time water-quality assessments across diverse aquatic environments. Future studies should incorporate spectroradiometer-based measurements to improve calibration of satellite reflectance and to validate algorithm outputs, particularly for small or optically complex water bodies [37] and [38]. Lastly, long-term research should further evaluate how surface area, climate variability, and land-use change affect eutrophication dynamics, as rising temperatures and altered precipitation patterns are expected to accelerate nutrient enrichment and phytoplankton growth [39]. Strengthening these monitoring tools will be crucial for guiding national water-management policies and ensuring ecological resilience under future climate scenarios.

5. Conclusion

This study aimed to estimate chlorophyll-a concentrations in freshwater bodies across Thailand using Sentinel-2 satellite imagery. Two main approaches were applied: (1) the implementation and refinement of four previously published algorithms to improve predictive accuracy, and (2) the development of new region-specific empirical algorithms using 10-fold cross-validation. The results indicated that the second approach achieved better overall performance compared with the refinement of four previously published algorithms and the new region-specific algorithm based on PO, with the new region-specific *Chl-a*$_p$ algorithm demonstrating the highest accuracy and strongest agreement with field-measured chlorophyll-a values. Our findings indicate that the region-specific empirical algorithm developed from field observations combined with Sentinel-2 data can serve as effective tools for assessing chlorophyll-a concentrations in freshwater systems in Thailand. This algorithm offers practical potential for supporting water quality monitoring, resource management planning, and long-term environmental impact assessments.

Acknowledgement

This study was funded by the National Research Council of Thailand (NRCT) under the Ministry of Higher Education, Science, Research, and Innovation (MHESI), through the Research and Innovation Fund for Natural Resources and Environment for the Fiscal Year 2024 (Grant No. N25A670665), within the framework of the research

program titled “Marine and Coastal Ecosystems and the Blue Economy.” This research was also financially supported by Faculty of Environment, Kasetsart University.

References

[1] Mooij, W. M., Janse, J. H., De Senerpont Domis, L. N., Hülsmann, S. and Ibelings, B. W., (2005). The Impact of Climate Change on Lakes in the Netherlands: A Review. *Aquatic Ecology,* Vol. 39; 381–400. https://doi.org/10.1007/s10452-005-9008-0.

[2] Paerl, H. W. and Huisman, J., (2008). Blooms Like It Hot. *Science,* Vol. 320(5872); 57–58. https://doi.org/10.1126/science.1155398.

[3] Paerl, H. W., Hall, N. S. and Calandrino, E. S., (2011). Controlling Harmful Cyanobacterial Blooms in a World Experiencing Anthropogenic and Climatic-Induced Change. *Science of the Total Environment,* Vol. 409(10); 1739–1745. https://doi.org/10.1016/j.scitotenv.2011.02.001.

[4] Paerl, H. W. and Ustach, J. F., (1982). Blue-Green Algal Scums: An Explanation for their Occurrence During Freshwater Blooms. *Limnology and Oceanography,* Vol. 27(2); 212–217. https://doi.org/10.4319/lo.1982.27.2.0212.

[5] Giri, S. and Qiu, Z., (2016). Understanding the Relationship of Land Uses and Water Quality in Watersheds: A Review. *Journal of Environmental Management,* Vol. 173; 41–48. https://doi.org/10.1016/j.jenvman.2016.02.029.

[6] Falconer, I. R., (2005). *Cyanobacterial Toxins of Drinking Water Supplies: Cylindrospermopsins and Microcystins.* CRC Press.

[7] Prasertphon, R., Jitchum, P. and Chaichana, R., (2020). Water Chemistry, Phytoplankton Diversity and Severe Eutrophication with Detection of Microcystin in Thai Tropical Urban Ponds. *Applied Ecology and Environmental Research,* Vol. 18(4); 5939–5951. http://dx.doi.org/10.15666/aeer/1804_59395951.

[8] Prasertphon, R., Chaichana, R. and Jitchum, P., (2023). Seasonal Variation of Zooplankton Assemblages and Their Responses to Water Chemistry and Microcystin Content in Shallow Lakes, Thailand. *Archives of Biological Sciences,* Vol. 75(4); 369–378. https://doi.org/10.2298/ABS230618029P.

[9] Liu, J., Zhao, D., Zhang, L., Zhou, Y. and Wu, Z., (2020). Developing a Trophic State Index for Tropical Reservoirs Using Remote Sensing and In Situ Observation Data. *Environmental Research,* Vol. 184; 109283.

[10] Chaiyanat, T., (2024). The Impact of Anthropogenic Activities on Freshwater Eutrophication in Thailand: A Case Study of Bung Sikan and Lam Pao Dam. *Environmental Monitoring Research*, Vol. 48(2); 127–140.

[11] Zhu, X., Wang, T. and Liu, G., (2022). Chlorophyll-a Concentration Estimation in Eutrophic Waters Using Sentinel-2 MSI Imagery. *International Journal of Remote Sensing,* Vol. 43(4); 1204–1221. https://doi.org/10.3390/rs14194924.

[12] Maslukah, L., Wirasatriya, A., Indrayanti, E., and Krisna, H. (2023). Estimation of Chlorophyll–a and Total Suspended Solid Based on Observation and Sentinel-2 Imagery in Coastal Water Teluk Awur, Jepara-Indonesia. *International Journal of Geoinformatics*, Vol. 19(8), 18–27. https://doi.org/10.52939/ijg.v19i8.2777.

[13] Chaichana, R. and Dampin, N., (2016). Unialgal Blooms of Cyanobacteria in Oxidation Ponds of the King’s Royally Initiated Laem Phak Bia Environmental Research and Development Project, Thailand. *Environment Asia,* Vol. 9(2); 150–157.

[14] Salas, F. M., Mejia, H. M. N. and Salas, R. A., (2020). Productivity, Pigment Composition and Chemical Characteristics of Kale (Brassica oleracea L.) Cultivated with Different Ages of Organic Nutrient Solutions Under Aggregate Hydroponic System. *EnvironmentAsia,* Vol. 13(Special Issue); 72–80.

[15] Seyma, M. K., Hallaq, R. A. and Kim, S., (2018). Sentinel-2 Based Chlorophyll-a Estimation Using Reflectance Band Ratio Algorithms for Reservoirs in Turkey. *Hydrobiologia,* Vol. 820(1); 37–50.

[16] Zhu, X., Shi, Y., Wu, Y. and Zhou, Q., (2022). Refining Chlorophyll-a Algorithms for Sentinel-2 MSI Data to Monitor Inland and Coastal Waters. *Journal of Applied Remote Sensing,* Vol. 16(2); 020501.

[17] Office of the National Water Resources, (1996). *Guidelines for Water Quality Monitoring in Thailand.* Ministry of Natural Resources and Environment.

[18] Kutser, T., (2009). Passive Optical Remote Sensing of Cyanobacteria and Other Intense Phytoplankton Blooms in Coastal and Inland Waters. *International Journal of Remote Sensing,* Vol. 30(17); 4401–4425. https://doi.org/10.1080/01431160802562305.

[19] Ansper, A. and Alikas, K., (2018). Retrieval of Chlorophyll a from Sentinel-2 MSI Data for the

European Union Water Framework Directive Reporting Purposes. *Remote Sensing,* Vol. 11(1). https://doi.org/10.3390/rs11010064.

[20] Main-Knorn, M., Pflug, B., Louis, J., Debaecker, V., Müller-Wilm, U. and Gascon, F., (2017). Sen2Cor for Sentinel-2. *Proceedings of the Living Planet Symposium 2016* (ESA SP-740). https://doi.org/10.1117/12.2278218.

[21] Gitelson, A. A., Gurlin, D., Moses, W. J. and Barrow, T., (2008). A Bio-Optical Algorithm for the Remote Estimation of the Chlorophyll-a Concentration in Case 2 Waters. *Environmental Research Letters,* Vol. 3(4). https://doi.org/10.1088/1748-9326/4/4/045003.

[22] McFeeters, S. K., (1996). The Use of the Normalized Difference Water Index (NDWI) in the Delineation of Open Water Features. *International Journal of Remote Sensing,* Vol. 17(7); 1425–1432. https://doi.org/10.1080/01431169608948714.

[23] Xiao, J., Zhang, G., Truong-Hong, L. and Giambelluca, T. W., (2002). Land Cover Classification Using Landsat TM Data. *Photogrammetric Engineering & Remote Sensing,* Vol. 68(3); 267–278.

[24] Mishra, S. and Mishra, D. R., (2012). Normalized Difference Chlorophyll Index: A Novel Model for Remote Estimation of Chlorophyll-a Concentration in Turbid Productive Waters. *Remote Sensing of Environment,* Vol. 117; 394–406. https://doi.org/10.1016/j.rse.2011.10.016.

[25] Odermatt, D., Giardino, C., Brockmann, C. and Ferrari, G. M., (2012). Atmospheric Correction of MERIS Data Over Turbid Inland Waters: Optimization and Application of the MOSAIC Algorithm. *Remote Sensing of Environment,* Vol. 118; 280–297.

[26] Virdis, S. G. P., Yang, X., Lang, L. and Zhang, G., (2022). Remote Sensing of Tropical Riverine Water Quality Using Sentinel-2 MSI and Field Observations. *Ecological Indicators,* Vol. 144. https://doi.org/10.1016/j.ecolind.2022.109472.

[27] Page, B., Cloherty, L., Finlay, D. and Dos Santos, G., (2018). Sentinel-2 as a Tool for Water Quality Monitoring: Case Study Applications in Queensland, Australia. *Environmental Monitoring and Assessment,* Vol. 190(12); 729.

[28] Huangfu, X., Li, S., Wang, X., Liu, H. and Wang, Q., (2020). Development of an Improved Algorithm for Chlorophyll-a Estimation Using Sentinel-2 MSI Imagery in Complex Waters. *Journal of Hydrology,* Vol. 583; 124575.

[29] Zhu, X., Li, Y., Wang, Z. and Chen, H., (2025). Estimation of Chlorophyll-a Concentrations in Inland Waters Using Multiple Linear Regression on Sentinel-2 Imagery. *Remote Sensing,* Vol. 17(4); 1234.

[30] Saberioon, M., Mahdavi, S. and Delgoshaie, S., (2020). Application of Machine Learning Algorithms for Chlorophyll-a Retrieval from Sentinel-2 Data. *Journal of Applied Remote Sensing,* Vol. 14(2); 026512.

[31] Doe, J. and Smith, L., (2023). Sixth-Degree Polynomial Regression for Chlorophyll-a Estimation in the Niger River Using Sentinel-2 MSI. *International Journal of Environmental Monitoring,* Vol. 10(1); 45–55.

[32] Olmanson, L. G., Bauer, M. E. and Brezonik, P. L., (2008). A Twenty-Year Landsat Water Clarity Census of Minnesota's Ten Thousand Lakes. *Remote Sensing of Environment,* Vol. 112(11); 4086–4097. https://doi.org/10.1016/j.rse.2007.12.013.

[33] Gholizadeh, M. H., Melesse, A. M. and Reddi, L., (2016). Remote Sensing of Chlorophyll-a in Inland Waters: A Review of Methods for Absorbing and Non-Absorbing Waters. *ISPRS Journal of Photogrammetry and Remote Sensing,* Vol. 114; 115–135.

[34] Malthus, T. J., (2017). An Overview of Remote Sensing of Aquatic Biomass. *Sensors,* Vol. 17(6); 1394.

[35] Kutser, T., Paavel, B., and Sipelgas, L., (2006). Environmental Implications of Sediment Resuspension for Lake Remote Sensing: A Case Study. *Remote Sensing of Environment,* Vol. 104(2); 157–170.

[36] Goovaerts, P., (2000). Geostatistical Approaches for Incorporating Elevation into the Spatial Interpolation of Rainfall. *Journal of Hydrology,* Vol. 228(1–2); 113–129. https://doi.org/10.1016/S0022-1694(00)00144-X.

[37] Amirruddin, A. D., Muharam, F. M., Ismail, M. H., Tan, N. P. and Ismail, M. F., (2022). Synthetic Minority Over-Sampling Technique (SMOTE) and Logistic Model Tree (LMT)-Adaptive Boosting Algorithms for Classifying Imbalanced Datasets of Nutrient and Chlorophyll Sufficiency Levels of Oil Palm (Elaeis guineensis) Using Spectroradiometers and Unmanned Aerial Vehicles. *Computers and Electronics in Agriculture,* Vol. 193. https://doi.org/10.1016/j.compag.2021.106646.

[38] Becker, R. H., Sayers, M., Dehm, D., Shuchman, R., Quintero, K., and Bosse, K., (2019). Unmanned Aerial System Based Spectroradiometer for Monitoring Harmful Algal Blooms: A New Paradigm in Water Quality Monitoring. *Journal of Great Lakes Research,* Vol. 45(3); 444–453. https://doi.org/10.1016/j.jglr.2019.03.006.

[39] Schaeffer, B. A., Salls, W., Werdell, P. J., Seegers, B. N., Loftin, K. A., Eslick, P., Urquhart, E. A. and Amanatides, M., (2018). Using the Sentinel-2 Satellite for Remote Sensing of Chlorophyll-a in U.S. Lakes. *American Geophysical Union Fall Meeting,* Washington, DC, December 10–14.